

Controlled Propulsion of Artificial Magnetic Nanostructured Propellers

Ambarish Ghosh[†] and Peer Fischer*

Rowland Institute at Harvard, Harvard University, Cambridge, Massachusetts 02142

Received January 19, 2009; Revised Manuscript Received March 27, 2009

ABSTRACT

For biomedical applications, such as targeted drug delivery and microsurgery, it is essential to develop a system of swimmers that can be propelled wirelessly in fluidic environments with good control. Here, we report the construction and operation of chiral colloidal propellers that can be navigated in water with micrometer-level precision using homogeneous magnetic fields. The propellers are made via nanostructured surfaces and can be produced in large numbers. The nanopropellers can carry chemicals, push loads, and act as local probes in rheological measurements.

Considerable progress has been achieved in manipulating nanoscale objects¹ on surfaces² and in high-vacuum environments. Attaining a similar level of control in fluidic environments^{3–7} could revolutionize many aspects of nanotechnology and open exciting possibilities in microfluidics and nanorheology. At microscopic length scales and therefore at low Reynolds numbers, reciprocal motion is absent as a potential means of locomotion (Scallop theorem⁸). Special swimming strategies are therefore needed. While propulsion in liquid crystal films,⁹ with electric fields,¹⁰ in magnetic field gradients,¹¹ and with the aid of chemical decompositions^{7,12} have been investigated, those that rely on a homogeneous magnetic field are especially promising as they can be operated from a distance in aqueous environments. Of particular scientific and technological interest are therefore magnetically actuated nano- and microstructures that “swim” similar to biological micro-organisms.^{13,14} Two strategies that permit swimming at low Reynolds number and that are used by living organisms are the flexible oarlike motions of spermatozoa and the cork-screw motion of bacterial flagella. Recently, the motion of spermatozoa was mimicked in an artificial magnetic swimmer of dimensions around 30 μm that executed some linear motion.⁴ A variety of cork-screws have also been fabricated^{5,15,16} with lengths from 30 μm to centimeters and have been moved linearly.

Here we describe a simple method of producing large numbers of nanostructured propellers and demonstrate the first fully controlled artificial swimmer that can be navigated with micrometer-level precision. Small size of artificial structures is especially beneficial, since colloidal length scales permit navigation in confined geometries and imply long sedimentation times. The propellers are typically 200–300 nm in width and about 1 to 2 μm long; they are driven by a homogeneous

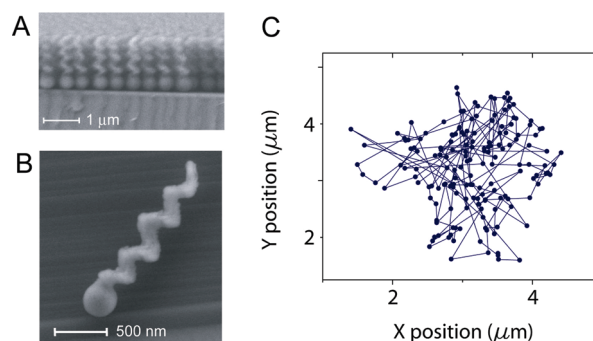


Figure 1. (A) SEM image of a wafer section with a nanostructured film containing $\sim 10^9$ SiO_2 helices/ cm^2 . (B) SEM image of an individual glass screw with nanostructured helicity. (C) Translational Brownian motion is observed in a 25 s trajectory of a single colloidal glass propeller in water (recorded at 7 frames/s).

magnetic field. They are made of silicon dioxide (SiO_2) and are thus easily functionalized. Despite being Brownian in the absence of a driving force, their motion can be fully controlled when a small magnetic field is applied.

To fabricate the glass (SiO_2) nanostructured propellers, we use a shadow-growth method, known as glancing angle deposition,¹⁷ which permits the growth of a wide variety of nanostructured thin films, including helical screwlike structures. A Si wafer (2 in. diameter) was first covered with a monolayer of silica beads of diameter 200–300 nm. The glass helices were then grown on the Si wafer by vapor deposition in an electron beam evaporator at a process pressure of 10^{-6} Torr. The SiO_2 vapor flux was incident at 87° and $\sim 3 \text{ \AA/s}$, while the wafer was rotated about its surface normal at ~ 0.07 rpm by a computer-controlled substrate manipulator. A wafer section of a vapor-deposited film with $\sim 10^9$ SiO_2 helical propellers per cm^2 is shown in Figure 1A. The helices are freed from the wafer by sonication and laid onto a surface. A thin layer (30 nm) of a ferromagnetic

* Corresponding author, fischer@rowland.harvard.edu.

[†] E-mail address: ghosh@rowland.harvard.edu.

material (cobalt) is deposited by thermal evaporation onto the surface and hence one-half of the helices. The substrate with the cobalt-covered helices is then placed between the pole pieces of an electromagnet, and the helices are magnetized, such that their magnetic moment is perpendicular to their long-axis (see also Supporting Information). A scanning electron microscopy (SEM) image of a single glass propeller is depicted in Figure 1B. To be able to track the swimmers, we coupled a fluorophore to the SiO₂ surface by mixing ~10 mg of (3-aminopropyl)dimethylethoxysilane (United Chemical Technology) with ~1 mg of Rhodamine B isothiocyanate (Aldrich) in 1 mL of dry ethanol at room temperature. In the absence of an external magnetic field, the propellers exhibit Brownian motion in water as can be seen in Figure 1C.

A triaxial Helmholtz coil is used to generate a homogeneous magnetic field of ~50 G rotating at frequencies of up to 170 Hz, with full directional control in all three dimensions. The permanent magnetic moment of the colloid strongly couples with the rotating magnetic field of the coil, and for each rotation the helix executes about its body axis, it translates forward or backward by its pitch, depending on its helicity and the sense of rotation of the magnetic field. That rotation about the long axis is favored, follows from the respective rotational drag coefficients, which may be estimated if one takes the nanoswimmers to be approximately ellipsoidal. The ratio f , of the drag about the major axis a relative to the minor axis b ratio is then given by¹⁸

$$f = \frac{2b^2}{a^2} \left[\ln\left(\frac{2a}{b}\right) - \frac{1}{2} \right] \quad (1)$$

where the dimensions are such that $a^2 \gg b^2$. The ratio of the drag coefficients for the lengths of 1–2 μm is $f \sim 0.1$, implying that rotation about the long axis is 10 times more efficient.

We can directly visualize the rotation/translation coupling in a single chiral colloid, as the magnetic layer, which only covers half of the body, is opaque, so that the fluorescence intensity is modulated as the screw rotates: bright as the dye faces the observer and dark when the magnetic film shields the dye. Two full rotations and the associated changes in fluorescence intensity are shown in the image sequence in Figure 2, where for each revolution, the swimmer propels through solution by 212 nm. The full movie is available as Supporting Information.

Once driven with a rotating magnetic field, strong rotation/translation coupling was observed, such that the nanostructured swimmer moves forward by its full pitch, for each rotation it executes about its body axis. The torque due to the magnetic field was stronger than the viscous drag due to the environment, such that the rotation matched the rotational frequency of the applied rotating magnetic field for the entire frequency range (dc to 170 Hz) of our coil. For frequencies around 150 Hz, the chiral colloids can be propelled at speeds of ~40 $\mu\text{m/s}$. It is interesting to note that the artificial swimmers of this Letter not only are similar in size to a bacterial cell but also move at similar speeds.

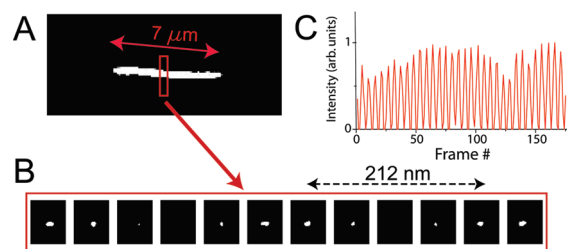


Figure 2. Images from a high-frame rate (low-resolution) video recording of (A) 0.5 s trajectory (recorded at 350 fps) and (B) individual images for a section of that trajectory. The swimmer is driven by a 60 G (6 mT) magnetic field rotating at 66 Hz in the plane orthogonal to its direction of translation. (C) In the total distance of 7 μm traversed by the swimmer at 14 $\mu\text{m/s}$, it blinks 33 times, such that each full rotation corresponds to a forward movement of 212 nm through solution. The corresponding movie is available as Supporting Information.

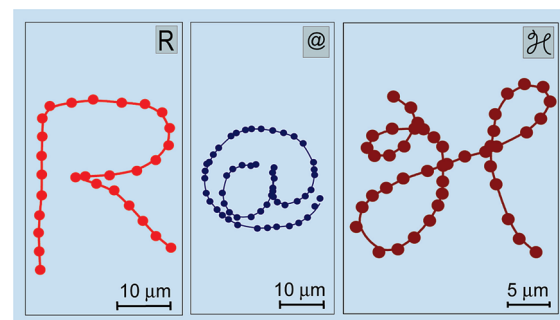


Figure 3. Trajectories of individual nanoswimmers in solution that navigate the preprogrammed “R@H” tracks that are shown in the insets. The points correspond to the position of the swimmer for each frame of the corresponding movie, while the lines show the entire track. The three corresponding movies and further details are available as Supporting Information.

Apart from size and speed, a technologically important aspect of any nanopropulsion scheme is the degree with which the motion can be controlled. Since Brownian motion tends to dominate at these length scales it is important for the effect of the magnetic field, B , on the permanent magnetic moment, μ , of the colloid to be much stronger than thermal motion, i.e., $\mu B \gg kT$, which is satisfied in the present system (see Supporting Information). The level of control observed with field strengths of 60 G can be seen in Figure 3, where we show the preprogrammed paths (inset) and the actual trajectory of a nanoswimmer in solution. The agreement can be seen to be excellent.

The swimmers with nanostructured chirality we describe could find applications in rheological measurements at the micro- and the nanoscale^{19–21} and could either be used as passive local probes or for active manipulation at these length scales. This is demonstrated in Figure 4A where a 1.5 μm long swimmer is driven against a silica bead a thousand times its volume and pushes it out of the field of view of the microscope. Standard microrheological techniques used to manipulate small particles, such as optical tweezers or atomic force microscopy (AFM), do not work at long range as they require proximity to a microscope objective or an AFM tip, respectively, whereas the nanoswimmers are readily controlled from a distance as the driving field is homogeneous. We estimate the force, F , which can be generated by a

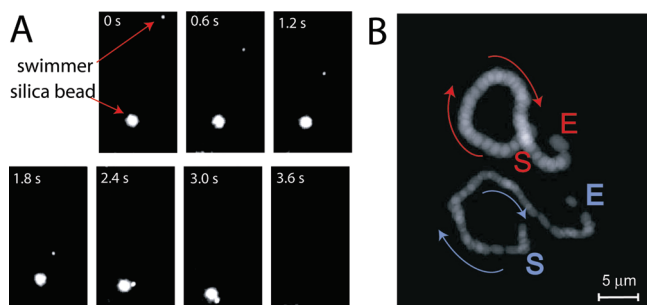


Figure 4. (A) A silica bead (5 μm diameter) is being pushed by a swimmer (1.5 μm long, 200 nm wide). The images (from left to right) show how the swimmer approaches the bead and pushes it out of the field of view. A 40 \times microscope objective was used, and the time gap between consecutive images is about 0.6 s. (B) Compound image of two swimmers follow identical paths under the action of a magnetic field preprogrammed to follow a curved trajectory from start (S) to end (E). The corresponding movie files are available as Supporting Information.

swimmer from the drag it overcomes (taking its shape to be approximately ellipsoidal):¹⁸

$$F = \frac{4\eta\pi av}{\left[\ln\left(\frac{2a}{b}\right) - \frac{1}{2}\right]} \quad (2)$$

where a and b are the dimensions along the major and minor axes, respectively, η is the viscosity of the surrounding medium, and v is speed of the swimmer. For a 2 μm long helix with a diameter of 200 nm traveling at 40 $\mu\text{m/s}$ in water, the generated force (\sim piconewtons) is comparable to a weak optical trap. However, the diameter of the swimmer is approximately 200 nm, and this results in a large applied pressure (\sim a few newtons per square meter), which could be advantageous for local manipulation, such as at biological membranes.^{22,23}

For certain applications in microfluidics,²⁴ as well as in drug delivery, it may be important to be able to manipulate more than one propeller simultaneously. That this is possible is demonstrated in the image in Figure 4B, where the tracks of two swimmers are seen that are simultaneously propelled with a high degree of control.

In summary, we have described the construction and operation of one of the smallest artificial swimmers to date. Due to their inherent chirality, the nanostructured swimmers presented in this Letter exhibit full coupling in their rotational and translational motions²⁵ and also make it possible to directly probe the use of hydrodynamic forces, such as shear²⁶ or vorticity²⁷ as a means of chiral separation. The fabrication method used to make the nanostructured helices can be used with a variety of materials and lends itself to large scale production. A variety of materials could be used; however, the fabrication of glass propellers permits molecules to be easily attached to the SiO₂ body of the swimmer via standard silane coupling chemistry. The propulsion mechanism is similar to that of a rotating flagellum of a bacterial cell, where now the rotation of the chiral colloid is controlled using a homogeneous magnetic field. This allows the propellers to be powered from a distance and permits full control in three dimensions. We expect that the simple method of realizing chiral colloidal swimmers in large numbers and the precise way with which they can be moved through solution will open up exciting possibilities and applications in microfluidics and nanorheological studies and in

delivering and mixing of chemicals and allow the potential use of artificial swimmers for biomedical applications to be explored.

Acknowledgment. The authors thank Frans Spaepen and Linda Stern for helpful suggestions, Gary Widiger for assistance with the chemistry, and the Rowland Institute of Harvard for financial support. This work was performed in part at the Center for Nanoscale Systems (CNS), a member of the National Nanotechnology Infrastructure Network (NNIN), which is supported by the National Science Foundation under NSF Award No. ECS-0335765. C.N.S. is part of the Faculty of Arts and Sciences at Harvard University.

Supporting Information Available: Description of experimental details and further information regarding the materials and methods used and movies: movie 1 showing object trajectory (slowed down 50 times and frames from this movie can be seen in Figure 2), movies 2, 3, and 4 showing the swimmer following the “R”, “@”, and “H” trajectories of Figure 3 (the magnetic field strength is \sim 60 G and the magnetic field vector rotates at frequencies ranging from 50 to 80 Hz), and movies 5 and 6 corresponding to parts A and B of Figure 4, respectively. This material is available free of charge via the Internet at <http://pubs.acs.org>.

References

- (1) Requicha, A. A. G. *Proc. IEEE* **2003**, *91*, 1922–1933.
- (2) Shirai, Y.; Osgood, A. J.; Zhao, Y.; Kelly, K. F.; Tour, J. M. *Nano Lett.* **2005**, *5*, 2330–2334.
- (3) Chang, S. T.; Paunov, V. N.; Petsev, D. N.; Veleev, O. D. *Nat. Mater.* **2007**, *6*, 235–240.
- (4) Dreyfus, R.; Baudry, J.; Roper, M. L.; Fermigier, M.; Stone, H. A.; Bibette, J. *Nature* **2005**, *437*, 862–865.
- (5) Ishiyama, K.; Sendoh, M.; Yamazaki, A.; Arai, K. I. *Sens. Actuators, A* **2001**, *91*, 141–144.
- (6) Jager, E. W. H.; Inganas, O.; Lundstrom, I. *Science* **2000**, *288*, 2335–2338.
- (7) Paxton, W. F. *J. Am. Chem. Soc.* **2004**, *126*, 13424–13431.
- (8) Purcell, E. M. *Am. J. Phys.* **1977**, *45*, 3–11.
- (9) Eelkema, R.; Pollard, M. M.; Vicario, J.; Katsonis, N.; Ramon, B. S.; Bastiaansen, C. W. M.; Broer, D. J.; Feringa, B. L. *Nature* **2006**, *440*, 163–163.
- (10) Osada, Y.; Okuzaki, H.; Hori, H. *Nature* **1992**, *355*, 242–244.
- (11) Pamme, N. *Lab Chip* **2006**, *6*, 24–38.
- (12) Ismagilov, R. F.; Schwartz, A.; Bowden, N.; Whitesides, G. M. *Angew. Chem., Int. Ed.* **2002**, *41*, 652–654.
- (13) Taylor, G. I. *Proc. R. Soc. London, Ser. A* **1951**, *209*, 447–461.
- (14) Berg, H. C.; Anderson, R. A. *Nature* **1973**, *245*, 380–382.
- (15) Zhang, L.; Abbott, J. J.; Dong, L.; Kratochvil, B. E.; Bell, D.; Nelson, B. J. *Appl. Phys. Lett.* **2009**, *94*, 064107–3.
- (16) Bell, D. J.; Leutenegger, S.; Hammar, K. M.; Dong, L. X.; Nelson, B. J. In *IEEE International Conference on Robotics and Automation*, 2007, 1128–1133.
- (17) Brett, M. J.; Hawkeye, M. M. *Science* **2008**, *319*, 1192–1193.
- (18) Berg, H. C. *Random Walks in Biology*; Princeton University Press: Princeton, NJ, 1983.
- (19) Waigh, T. A. *Rep. Prog. Phys.* **2005**, *68*, 685–742.
- (20) Cicuta, P.; Donald, A. M. *Soft Matter* **2007**, *3*, 1449–1455.
- (21) Squires, T. M.; Brady, J. F. *Phys. Fluids* **2005**, *17*, 073101–21.
- (22) Weihs, D.; Mason, T. G.; Teitell, M. A. *Biophys. J.* **2006**, *91*, 4296–4305.
- (23) Cai, D.; Mataraza, J. M.; Qin, Z.-H.; Huang, Z.; Huang, J.; Chiles, T. C.; Carnahan, D.; Kempa, K.; Ren, Z. *Nat. Methods* **2005**, *2*, 449–454.
- (24) Terray, A.; Oakey, J.; Marr, D. W. M. *Science* **2002**, *296*, 1841–1844.
- (25) Han, Y.; Alsayed, A. M.; Nobili, M.; Zhang, J.; Lubensky, T. C.; Yodh, A. G. *Science* **2006**, *314*, 626–630.
- (26) Makino, M.; Doi, M. *Phys. Fluids* **2005**, *17*, 103605.
- (27) Kostur, M.; Schindler, M.; Talkner, P.; Hanggi, P. *Phys. Rev. Lett.* **2006**, *96*, 014502.

NL900186W